Performance Evaluation of a Rib-Reinforced Culvert

ERNEST T. SELIG and SAMUEL C. MUSSER

ABSTRACT

A circumferential rib-reinforced long-span culvert was constructed and its performance evaluated by means of field measurements and a limited finite-element analysis. Results were compared with current design practice. The structural design was shown to considerably exceed the requirements of the American Iron and Steel Institute and AASHTO; in fact, the analysis suggested that neither ribs nor other special features were necessary. Ribs were shown to be beneficial, however, in improving buckling resistance and in controlling deflections during backfilling. Finally, finite-element methods of analysis were concluded to be useful by permitting moments to be incorporated into the design considerations.

One of two accepted special features for long-span culverts mentioned by AASHTO is circumferential rib stiffeners. An example of a culvert with such rib stiffeners is one fabricated by Syro Steel Company and constructed in Sacramento County, California, in May 1983. This structure has formed the basis for a study of the performance of rib-stiffened culverts. A synopsis of the results is given in this paper.

INSTALLATION DESCRIPTION

The completed configuration is shown in Figure 1. The culvert is a horizontal ellipse with 23 ft (7 m) of span and 14 ft 1 in. (4.3 m) of rise fabricated from 10-gauge, 6 x 2-in. (152 x 51-mm) corrugated steel bolted plates. Steel angle ribs [3 x 3 x 1/4 in. (76 x 76 x 6 mm)] extending over the top from springline to springline were attached at 3-ft (0.9-m) intervals along the length.

The natural soil (zone A in Figure 1) was a heterogeneous system with layers of loosely cemented sandstone, alluvial silt, and granular river dredgings that contained sizes up to boulders. This existing ground was first excavated to about 1 ft (0.3 m) below the invert elevation; then a crushed rock [less than 3/4-in. (19-mm) size] was placed as bedding (zone B). The bedding was shaped to the bottom of the ellipse and extended to an elevation of about 2 ft (0.6 m) above the invert. The lower portion of the sidefill (zone C) consisted of the same crushed rock to a depth that varied along the length. The upper portion of sidefill (zone D) was sand that extended to about 1 ft over the crown. The final 2 ft of cover (zone E) was the granular river dredgings.

A minimum of 90 percent AASHTO T-180 maximum density was requested. The sidefill was compacted in lifts 6 to 8 in. (152 to 203 mm) thick to the top radius change by using a walk-behind vibratory roller. The remaining fill was placed in 12-in. (0.3-m) lifts and compacted with a smooth drum roller.

MEASUREMENTS

Deflections were obtained by triangulation with distances measured by taping between reference points around the inside of the structure. The deflections are believed accurate to within 0.1 in. (2.5 mm).

The final dead-load deflection with 3 ft of cover is shown in Figure 2. The change in span and rise with increasing fill height is shown in Figure 3. The final peaking is 1.75 in. (44 mm), but the maximum apparently was greater than 2 in. (51 mm) when the backfill was at the crown elevation. However, the shape of this portion of the curve is not certain because no deflection measurements were made during this stage of construction. A proper final shape is critical to good performance, and hence close monitoring of the shape during construction is important.

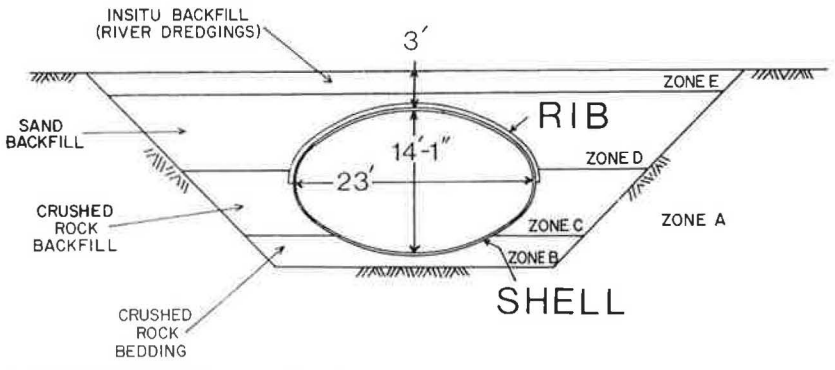

FIGURE 1 Installation configuration.

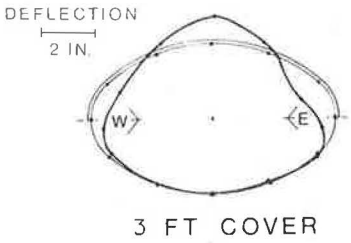

FIGURE 2 Measured dead-load deflections.

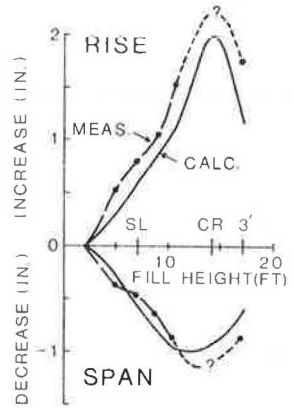

FIGURE 3 Measured dead-load thrust.

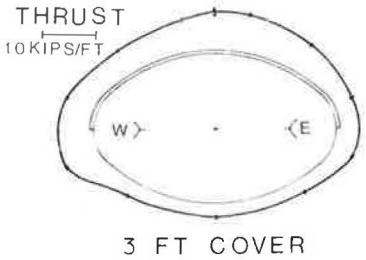

FIGURE 4 Measured dead-load moment.

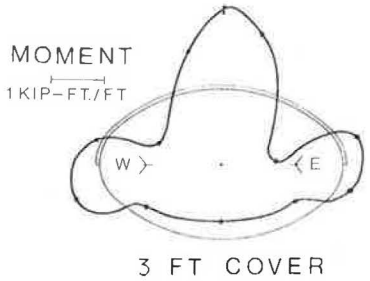

FIGURE 5 Comparison of measured and calculated dead-load deflections.

Bonded foil-type strain gauges, temperature compensated for steel, were placed on the corrugations near the ribs and also on the ribs to determine the circumferential thrust and bending moment around the ellipse. A three-wire, quarter-bridge circuit was used. The manufacturer's specified gauge factor was assumed correct. The circumferential stress was calculated from the circumferential strain assuming uniaxial stress conditions. The shell stresses were assumed to be uniform along the length of shell between ribs, that is, not influenced by the location of the ribs. The thrust and moment were then calculated from the measured circumferential stress distribution by using simplified cross-section geometry for the rib and corrugated shell. These values are believed to have an error of less than 10 to 20 percent.

Even though strain-gauge temperature compensation was intended, strain measurements made on sections of structure before they were covered by soil appeared to be inconsistent, probably as a result of the large temperature fluctuations. Thus the measured changes in dead-load thrust and moment with fill-height increase require further study and therefore have not been included.

The final dead-load thrust with 3 ft of cover is shown in Figure 4. The thrust shows a tendency to decrease with distance from the crown to the invert.

The final dead-load moment with 3 ft of cover is shown in Figure 5. The maximum moments occur at the crown and top quarter points. This trend has been found to be typical for both circumferentially and longitudinally stiffened flexible, long-span structures and arches (1-4). With longitudinal stiffeners, however, the maximum quarter-point moment has been observed to be shifted to either side of the stiffener device (2,3).

The points where these maximum moments occur are the probable locations of plastic hinge formation if the moment capacity of the structure is inadequate. When sufficient plastic hinges develop so as to create an unstable mechanism, snap-through buckling will likely result. On a full-barrelled structure such as the horizontal ellipse investigated here, three plastic hinges forming at the locations of maximum moment could result in such a failure mechanism. Note, however, that on open-bottomed arch structures two hinges, in addition to those at the footings, might be sufficient to create instability. Hence, adequate moment capacity should be provided at all points around the periphery to resist the probable formation of plastic hinges. This points out the importance of a generalized analysis technique that can predict the magnitude and distribution of bending moments around the periphery of structures with varying shapes.

COMPUTER ANALYSIS

A finite-element computer analysis was performed with CANDE (5) and NLSSIP (6), the latter program being similar to SSTIPN. Fully composite action between the rib and a 3-ft length of corrugated steel shell was assumed for determining the moment of inertia of the rib-stiffened portion of the structure. The steel component properties and material parameters were the usual values.

The soil was represented in the computer analysis by the hyperbolic Young's modulus and bulk modulus model (7). Hyperbolic parameters for the crushed rock and the sand were based on triaxial tests, whereas those for the river dredgings were estimated by using data from other soils. The triaxial tests showed that the stress-strain characteristics of the crushed rock and sand were very similar.

Incremental backfill layer placement was done in six steps after placement of the bedding and the structure. Thus placement of layers under the haunch

was included in the computer analysis even though past experience has shown that this is difficult to simulate. One problem is that part of the weight of soil elements in contact with the pipe is assigned to the pipe nodes. This has the effect of pulling down on the structure. Compensation for this effect was provided in CANDE by applying a compaction pressure. NLSSIP did not have the capability of applying compaction pressure, but this program was modified to avoid placing soil weight on the pipe. Even so, the full effect of placing, spreading, and compacting soil was not represented.

The compaction effect during layer placement was simulated in CANDE by using a method proposed by Katona (8). It involves applying a uniform pressure across the top of each layer when placed. As each succeeding layer is placed, a negative pressure is applied to the top of the previous layer to cancel the surface pressure on that layer. This also has the effect of squeezing the top layer each time. In this study compaction pressures were first applied to the bedding and ended at various elevations between the top quarter point and the ground surface. Generally the pressures were not included directly over the structure.

CANDE had the capability of permitting slip by assigning a coefficient of friction between the soil and the steel, which limits the shearing resistance. The NLSSIP program only provides full bonding.

Parametric computer studies were carried out with CANDE to evaluate the effect of variation of parameters. The main observations are as follows:

1. The main effect of the ribs was to significantly decrease (about 50 percent) final deflections. The final moments were greater with the ribs because of greater bending stiffness, but the thrust was essentially unaffected.
2. Allowing interface slip with limiting friction gave slightly greater final deflections.
3. Reducing the ring-compression stiffness by decreasing the bottom plate area by a factor of 6 to account for seam compression, as proposed by Chang et al. (9), did not significantly change the magnitudes of thrust, moment, and deflection but did give a thrust distribution more nearly like that in Figure 4.
4. Increasing soil stiffness decreased deflections and the crown moment. Increasing the soil Poisson's ratio significantly increased deflection during soil placement under the haunch.
5. Increasing the compaction pressure increased the final deflections. Increasing the elevation above the top quarter point at which compaction was stopped increased the final crown moment and decreased the final thrust. Also maximum peaking occurred at increasingly higher elevations as compaction was extended to higher elevations. The overall trends showed that a better method of compaction simulation is needed.

COMPARISONS WITH MEASUREMENTS

Without the compaction pressure, the NLSSIP analyses underestimated the measured deflections by a factor of at least 2. Thus only the CANDE results are compared with the measured values. No single CANDE computer analysis provided simultaneous agreement with all measured results. However, the parametric study results showed that overall agreement was best with the following conditions:

1. Ribs with fully composite action,
2. Slip only over the bottom half of the structure,
3. Steel area reduction factor of 1/6 over the bottom half of the structure to represent reduced ring compression stiffness from seam slip, and
4. Compaction pressure of 15 psi (103 kPa).

The following comparisons are based on the computer analysis incorporating these conditions.

A comparison of calculated and measured changes in rise and span as a function of fill height above the invert was shown in Figure 3. Although the final calculated deflections are smaller, the agreement is reasonable, especially considering the difficulty in modeling below the springline.

Live load was measured with a 50-ton (445-kN) vehicle that had five axles. Two groups of tandem axles formed the main loads over the structure; each axle weighed 11 to 12 tons (107 kN). This represents AASHTO's alternative military load, which is greater than HS 20 and twice the specified HS 15 design axle load. A concentrated load was used in CANDE to model each axle, and a full mesh was constructed so that all five axle loads could be applied. The magnitude of the concentrated load was obtained by dividing the axle load by 12 ft (3.7 m), which represents one lane width.

The calculated live-load thrust at the crown was about half the measured value of 5 kips/ft (73 kN/m) (1 kip = 4.5 kN):

	Thrust		
		Predicted (kips/ft)	
	Measured (kips/ft)	With Ribs	Without Ribs
Crown	5.0	2.2	2.2
Springline	0.4	1.5	1.5
Invert	0.0	0.6	0.7

Calculated thrusts at the springline and invert were higher than the measured values. Calculated values were essentially the same whether ribs were included or not; that is, the ribs did not cause any thrust increase.

The calculated live-load moment at the crown with the ribs present was about 5 times greater than the measured live-load moment of 0.3 kip-ft/ft (1.3 kN-m/m) (1 kip = 4.5 kN, 1 in. = 25 mm):

	Moment and Deflection		
		Predicted	
	Measured	With Ribs	Without Ribs
Crown (kip-ft/ft)	-0.3	-1.2	-0.6
Rise (in.)	-0.18	-0.38	-0.45
Span (in.)	+0.01	+0.10	+0.14

This is consistent with the larger calculated deflections. Thus, in terms of moment and deflection, the live load used appeared to be too large.

The live-load deflections calculated without the ribs present were about 30 to 40 percent greater than those with the ribs. The corresponding live-load moment calculated without the ribs was half the value with ribs. Thus, the increase in moment from increased deflection without ribs was more than offset by the decrease in moment from decreased bending stiffness. In other words, adding ribs reduces deflections but increases bending stress. This increase in bending stress is mitigated, however, by the increased bending capacity that ribs provide. In this case, the addition of ribs doubled the plastic moment capacity of the section.

As shown in Figure 2, construction operations resulted in peaking at the crown of 1.75 in. (44 mm) with 3 ft of cover. This type of controlled peaking is advantageous in that it pretensions the top arc

of the structure and provides a greater crown moment capacity safety factor against future overloads than would otherwise exist. Thus, although live-load thrust increased the magnitude of dead-load thrust, live-load moment cancelled part of the dead-load moment to produce a smaller maximum moment with the live load present than without it.

The calculated dead-load thrusts with the 3 ft of cover agreed closely with measured values (1 kip = 4.5 kN):

	Thrust				
		Predicted (kips/ft)			
	Measured (kips/ft)	Finite Element	$T = P_{CR}R_T$	$T = \gamma HS/2$	Full Weight
Crown	7.3	6.8	5.8	4.3	6.7
Springline	5.6	5.3	5.8	4.3	6.7

The dead-load thrust for non-long-span culverts is usually taken as equal to or less than the product of soil density, height of cover, and half the span. This significantly underestimates the thrust. The long-span thrust calculation of the American Iron and Steel Institute (AISI) (10) and AASHTO (11) is taken as equal to the product of soil density, height of cover, and crown radius of curvature. This was still low for the Sacramento culvert, but more reasonable. The final alternative, given as an option by AISI for long-span structures, is to use half of the full soil weight above the structure, not just that above the crown. This value is close to that calculated by the finite-element method and only slightly less than the measured maximum. Clearly, for determining the design thrust with the usual methods a significant negative arching is present. This has been shown before and is a result of the high ring-compression stiffness of bolted corrugated plate structures. Thus the bending flexibility reduces the crown pressure below the free-field or geostatic value (soil density times cover height), but not the thrust.

COMPARISONS WITH OTHER ANALYSIS METHODS

In Figure 6 the dead-load thrust trends of AISI (10) and AASHTO (11) and the proposed soil-culvert interaction (SCI) (1,12) design methods are compared with the average of crown and springline measured thrust at 3 ft of cover. The measured value is best represented by the alternative AISI method, which uses the full soil weight above the springline. The SCI method substantially overestimates dead-load thrust. On the other hand, the AISI and AASHTO methods, which use the top arc radius on long spans, underestimate dead-load thrust. It has been shown by Leonards et al., in a paper in this Record, that this trend of underprediction worsens with increasing rise/span ratios.

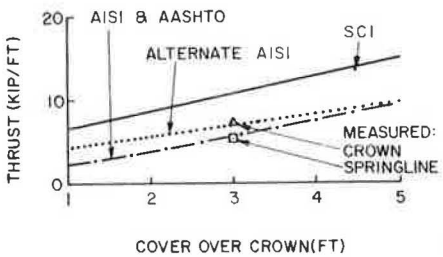

FIGURE 6 Design dead-load thrust compared with measured values ($\gamma = 0.134$ kip/ft^3 to 1 ft cover; $\gamma = 0.120$ kip/ft^3 above 1 ft cover).

A similar comparison for live-load thrust is given in Figure 7. Here, the alternative AISI and the SCI methods come closest to estimating the average of the crown and springline measured thrust. The usual AISI and AASHTO methods greatly overestimate the thrust. This trend worsens with decreasing cover.

The springline thrust calculated for the design methods shown in Figure 7 is based on an AASHTO HS 20 loading [32 kips (142 kN), single axle]. The measured values, on the other hand, resulted from the AASHTO alternative military loading [tandem axles, 24 kips (107 kN) each]. For the alternative AISI method, the unit live load was taken as equal to the concentrated axle load divided by the lane width. The SCI method uses a unit live load, which gives the same pressure at the crown elevation as the concentrated axle load, assuming a Boussinesq distribution. The older AISI and AASHTO methods apply the Boussinesq peak pressures at the crown elevation to the entire structure.

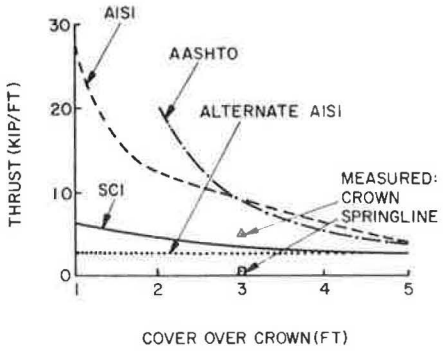

FIGURE 7 Design live-load thrust for HS 20 loading compared with measured values for military loading (impact factors omitted).

Only the generalized finite-element analysis and the proposed SCI design method provide an estimate of bending moments in flexible culverts. Comparisons of SCI's predictions for dead- and live-load moments with measured values are given in Figures 8 and 9. The SCI method assumes that the worst moment for design purposes occurs at the top quarter-span point when a live load is over the quarter point. The measured value shown represents this same situation. For moment calculations the SCI method also establishes a flexibility number that relates structural material and sectional properties to the stiffness of the soil and the span of the structure. The triaxial tests on the project soils suggested that they possessed closer to twice the in-place stiffness suggested by SCI for GW material with 100 percent T-99 relative compaction. For this reason, results for both soils are represented in Figures 8 and 9.

The SCI method underpredicted the measured value of dead-load moment at the quarter point (Figure 8), particularly when the measured project soil properties were used. This probably results from less predicted deformation during backfilling than actually occurred.

The SCI-predicted quarter-point live-load moment differed substantially from the measured live-load moment (Figure 9), even with the project soil properties. The SCI method predicted a moment increase with live-load application, whereas the actual effect of the live load was to slightly decrease the quarter-point moment. This is believed to be a direct result of the amount of crown peaking achieved during back-

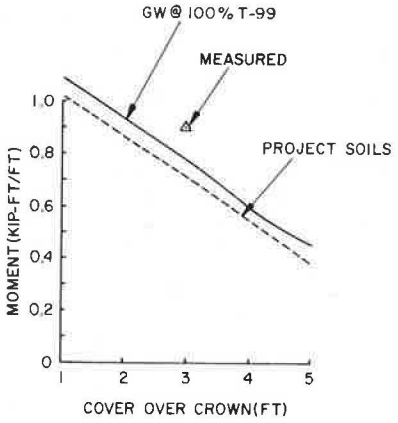

FIGURE 8 Design quarter-point dead-load moment for SCI method compared with measured value.

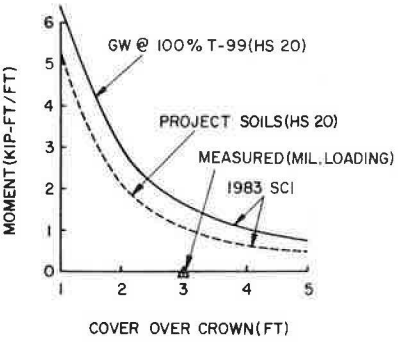

FIGURE 9 Design quarter-point live-load moment with load over quarter point for SCI method compared with measured value (impact factors omitted).

filling, which was not represented in the SCI analysis.

As noted earlier, the introduction of live loads on 3 ft of cover affected measured moments only slightly. Canadian studies also showed a relative insensitivity of moment to the introduction of live loads (13). This has been shown to be true for long-span structures, both with and without relieving slabs.

DESIGN CHECK OF MEASURED VALUES

Thrust measurements for the top half of the structure with ribs indicated that the factor of safety for average compressive stress against wall yield was greater than 6. If ribs had not been present, this factor of safety still would have exceeded 5. For the bottom half of the structure, which had no ribs, the factor of safety against wall yield exceeded 9. Note that these factors of safety were for live loads twice the magnitude of those specified for the design.

Although moments are not directly included in the AISI and AASHTO long-span design recommendations, they are important in the stability analysis of the structure and should not be ignored. They are more critical in structures with low rise/span ratios, shallow cover, unsymmetric loading, or less than ideal backfill materials. As pointed out earlier, the most critical moments for this structural configuration under shallow cover are the inward-acting ones at the quarter points. The maximum quarter-point moment, which was the value measured before the application of live load, was 1.1 kip-ft/ft (5 kN-m/m). With ribs, the factor of safety against plastic hinge formation at the quarter point exceeded 5. If an equivalent moment had occurred in the same structure without ribs, the safety factor would have been half that. Also, deflections would have increased somewhat.

The thrust and moment evaluation indicates that in this case ribs were not needed to satisfy structural mechanics considerations. In fact, no special features were needed except to satisfy the code requirements. Alternatively, a 12-gauge corrugation could have been used with wider rib spacing. It was the decision of Sacramento County to use the more conservative design.

CONCLUSIONS

For the Sacramento culvert, the performance at the end of construction considerably exceeded the structural design requirements. The field measurements indicate that performance would also have been satisfactory with no special features.

The circumferential ribs were found to have the following advantages:

1. They helped control shape and magnitude of deflections during backfill placement and compaction, and
2. They increased the factor of safety against plastic hinge formation, which leads to snap-through buckling.

Finite-element analysis is useful in designing large flexible corrugated-metal culverts. First, this approach permits an evaluation of the parameters influencing thrust, moment, and deflection. Second, the potential for snap-through buckling can be analyzed by using the estimated magnitudes of moments and probable locations of plastic hinge formation.

The older AISI and AASHTO methods were very conservative for predicting live-load thrust and slightly unconservative for dead-load thrust. The alternative AISI method gave reasonable values for the dead-load and live-load thrusts. The SCI method was very conservative for dead-load thrust but gave a reasonable value for live-load thrust.

The SCI method gave an unconservative but reasonable value for dead-load moment. However, the live-load moment from the SCI method was totally different from the measured maximum value, and very conservative. Thus, in its current form, the SCI method may not offer a general solution to the problem of live-load moments for all flexible structures.

ACKNOWLEDGMENT

The field measurements and data reduction were performed through a joint effort of Reynold Watkins and other Utah State University staff and by Samuel C. Musser of Syro Steel Company.

REFERENCES

1. J.M. Duncan. Behavior and Design of Long-Span Metal Culverts. Journal of the Geotechnical Engineering Division, ASCE, March 1979.
2. E.T. Selig, C.W. Lockhart, and R.W. Lautensleger. Measured Performance of Newtown Creek Culvert. Journal of the Geotechnical Engineering Division, ASCE, Sept. 1979.

3. M.C. McVay and E.T. Selig. Performance and Analysis of a Long-Span Culvert. In Transportation Research Record 878, TRB, National Research Council, Washington, D.C., 1982, pp. 23-29.
4. D.B. Beal. Behavior of Aluminum Structural Plate Culvert. In Transportation Research Record 878, TRB, National Research Council, Washington, D.C., 1982, pp. 100-104.
5. M.G. Katona, J.M. Smith, R.S. Odello, and J.R. Allgood. CANDE--A Modern Approach for the Structural Analysis of Buried Culverts. Report FHWA-RD-77-5. FHWA, U.S. Department of Transportation, Oct. 1976.
6. J.M. Duncan. Nonlinear Soil-Structure Interaction Program. University of California, Berkeley, undated.
7. J.M. Duncan, P. Byrne, K.S. Wong, and P. Mobry. Strength, Stress-Strain and Bulk Modulus Parameters for Finite Element Analysis of Stresses and Movements in Soil Masses. Report UCB/GT/80-01. University of California, Berkeley, Aug. 1980.
8. M.G. Katona, D.F. Meinhert, R. Orillac, and C.H. Lee. Structural Evaluation of New Concepts for Long-Span Culverts and Culvert Installations. Report FHWA-RD-79-115. FHWA, U.S. Department of Transportation, Dec. 1979.
9. C.S. Chang, J.M. Espinoza, and E.T. Selig. Computer Analysis of Newtown Creek Culvert. Journal of the Geotechnical Engineering Division, ASCE, Vol. 106, No. GT5, May 1980, pp. 531-556.
10. Handbook of Steel Drainage and Highway Construction Products. American Iron and Steel Institute, Washington, D.C., 1983.
11. Standard Specifications for Highway Bridges. AASHTO, Washington, D.C., 1977.
12. J.M. Duncan and R.H. Drawsky. Design Procedures for Flexible Metal Culvert Structures. Report UCB/GT/83-02, 2nd ed. Department of Civil Engineering, University of California, Berkeley, May 1983.
13. B. Bakht and Z. Knoble. Testing of a Soil Steel Structure with a Relieving Slab. Report SRR-84-4. Ministry of Transportation and Communication, Downsview, Ontario, Canada, Jan. 1984.

Publication of this paper sponsored by Committee on Culverts and Hydraulic Structures.